Energy-Dependent Photoemission Time Delays of Noble Gas Atoms Using Coincidence Attosecond Streaking

Claudio Cirelli, Mazyar Sabbar, Sebastian Heuser, Robert Boge, Matteo Lucchini, Lukas Gallmann, and Ursula Keller, *Fellow, IEEE*

(Invited Paper)

***Abstract*—We present photoemission time-delay measurements between electrons originating from the valence shells of neon and argon obtained by attosecond streaking. After giving a brief review of the different techniques, we focus on more detailed analysis using the attosecond streaking technique. We show that the temporal structure of the ionizing single attosecond pulse may significantly affect the obtained time delays, and we propose a procedure how to take this contribution properly into account. Our analysis reveals a delay of a few tens of attoseconds in a photon energy range between 28 and 40 eV in the emission of electrons ionized from argon with respect to those liberated from neon.**

***Index Terms*—Atomic physics, ultrafast optics, ultraviolet spectroscopy, time measurement.**

I. Introduction

RECENT progress in ultrafast science has lead to the generation and use of extreme ultra-violet (XUV) attosecond pulses [1], [2], providing the experimental tools for real-time observation of electron dynamics in atomic, molecular and solid targets [3]–[5]. The possibility to access dynamics in the subfemtosecond time domain opened up the opportunity to address new sets of physical problems. For instance a simple question that can be posed is how long does it take for light to remove an electron from an atom or a molecule? The answer to this question is not trivial because it is well known in quantum mechanics that time is not a direct observable quantity [6]. Therefore timing information has to be inferred indirectly by choosing other measurable observables.

The main experimental techniques that have addressed this question are the attoclock [7], [8], attosecond streaking [2], [9] and two-photon sideband (SB) interferometry, often referred to as the RABBITT (reconstruction of attosecond beating by interference of two-photon transitions) method [1], [10].

With photon energies well below the ionization potential of an atom a bound electron can be removed in the strong laser field interaction through multiphoton or tunnel ionization. A recent estimation of a tunneling delay time in helium [11], [12] has been obtained with the attoclock, which is a method well suited to study strong-field ionization dynamics. The technique employs only a single elliptically polarized few-cycle pulse [8]; the precise knowledge of the polarization state of the laser field determines the calibration of the clock, while the timing information with attosecond resolution is extracted by measuring the angular component of the electron momentum after ionization with great accuracy.

On the other hand with photon energies above the ionization potential, single-photon ionization dynamics can be investigated using either attosecond streaking or RABBITT with a pump-probe two-color scheme, where a relatively strong femtosecond infrared (IR) laser field is used at the target together with the attosecond pulses. In attosecond streaking, a single attosecond pulse (SAP) is used to ionize the target [2], [9], while in RABBITT attosecond pulse trains (APTs) are employed [1]. In both cases, the synchronized IR probe pulse provides the timing information.

RABBITT and attosecond streaking have been employed to measure the relative photoemission time delay between electrons emitted from two distinct energy levels of argon [13] and neon [14], respectively. Here, we extend the attosecond streaking method with coincidence detection, thus accessing the energy-dependent difference in photoemission time delay between electrons ionized from multiple atomic species within the same experiment thus assuring identical experimental conditions.

II. Time Delay Determination

Although our work presented here deals entirely with attosecond streaking measurements, let us first briefly review how timing information is retrieved using the RABBITT method. Most of the physical concepts are the same for both methods and the goal of our paper is to show how to adopt some precautions that are inherently employed in RABBITT also in streaking measurements.

Manuscript received January 14, 2015; revised March 18, 2015; accepted March 18, 2015. This work was supported by the ERC advance Grant ERC-2012-ADG_20120216 within the seventh framework program of the European Union and by the NCCR MUST, supported by the Swiss National Science Foundation.

C. Cirelli, M. Sabbar, S. Heuser, R. Boge, M. Lucchini, and U. Keller are with the Department of Physics, ETH Zurich, 8093 Zurich, Switzerland (e-mail: cirelli@phys.ethz.ch; msabbar@phys.ethz.ch; sheuser@phys.ethz.ch; rboge@phys.ethz.ch; mlucchini@phys.ethz.ch; keller@phys.ethz.ch).

L. Gallmann is with the Institute of Applied Physics, University of Bern, 3012 Bern, Switzerland, and also with the Department of Physics, ETH Zurich, 8093 Zurich, Switzerland (e-mail: gallmann@phys.ethz.ch).

Color versions of one or more of the figures in this paper are available online at http://ieeexplore.ieee.org.

Digital Object Identifier 10.1109/JSTQE.2015.2416152

1077-260X © 2015 IEEE. Translations and content mining are permitted for academic research only. Personal use is also permitted, but republication/redistribution requires IEEE permission. See http://www.ieee.org/publications_standards/publications/rights/index.html for more information.

A. RABBITT

In the case of RABBITT, the time delay in the atomic photo ionization process is contained in the phase of the SB oscillations, generated by the interference of two ionization channels, both involving absorption of a harmonic photon from the XUV frequency comb of the APT and the absorption (or emission) of an additional IR photon [15].

The total phase φ_{SB} of the SB oscillations is the sum of two main contributions: the phase difference between consecutive harmonics φ_{atto} and the so-called atomic phase $\varphi_{\mathrm{atomic}}$ due to the two-photon ionization process as previously described. Similar to the SPIDER measurements [16] a constant phase between all the harmonics results in an averaged transform-limited attosecond pulse within the APT. Thus a frequency-dependent phase φ_{atto} broadens the attosecond pulses and determines the average attochirp of the individual attosecond pulses within the ATP. Note that in this case no phase dependence within the individual harmonics is measured which would determine the APT duration.

The atomic phase $\varphi_{\mathrm{atomic}}$ is related to the intrinsic photoelectron group delay, which in turn may give access to the Eisenbud–Wigner–Smith (or also referred to as simply the Wigner) photoionization time delay [17], [18]. The latter is defined as the measure for the spectral variation of the scattering phase and represents the phase accumulated by the photoelectron when escaping the atomic Coulomb potential.

The propagation of the electron wavepacket can then be seen in terms of the linear phase shifts acquired by the individual monochromatic waves that result into a time delay with respect to the free propagation. This effect is analogous to the propagation of a laser pulse through a dispersive medium: in both cases, the group delay experienced by the electron wavepacket or the laser pulse is given by the derivative of the spectral phase ϕ at any frequency ω: $\tau = \partial\phi/\partial\omega$. More details will be given in Section III-D.

In principle, from a single RABBITT measurement it is not possible to disentangle the contributions of the two components φ_{atto} and $\varphi_{\mathrm{atomic}}$ to the total phase. Thus an additional reference measurement must be performed such as for electrons ionized from two different initial states [13] or from two different targets simultaneously [19]. Using the same APT for both RABBITT traces ensures that the contribution of the term φ_{atto} cancels out. Hence, the difference of the atomic phases results to be:

$$\Delta\varphi_{\mathrm{SB}} = \varphi_{\mathrm{SB}}^{(1)} - \varphi_{\mathrm{SB}}^{(2)} = \varphi_{\mathrm{atomic}}^{(1)} - \varphi_{\mathrm{atomic}}^{(2)}. \tag{1}$$

It is important to note that the SB oscillations around the same harmonic order have to be compared in both RABBITT traces to make sure that the liberated electrons have absorbed XUV photons of the same energy. Only in this case the phase difference due to the temporal structure of the APT φ_{atto} is the same and cancels out (1). For example a finite attochirp introduces a significant time delay between the different spectral components inside the attosecond pulse. Thus using different SBs will introduce an additional phase shift, which would not cancel out according to Eq. (1).

When this procedure is adopted, a photoionization delay difference $\Delta\tau_{\mathrm{atomic}}$ between the two initial states can be computed dividing the phase difference of SB oscillations by their modulation frequency given by the IR frequency ω_{IR}:

$$\Delta\tau_{\mathrm{atomic}} = \left(\delta\varphi_{\mathrm{atomic}}^{(1)} - \delta\varphi_{\mathrm{atomic}}^{(2)}\right)/2\omega_{\mathrm{IR}} = \Delta\varphi_{\mathrm{SB}}/2\omega_{\mathrm{IR}}. \tag{2}$$

In recent experiments, the delay between electrons emerging from 3p and 3s states in argon has been measured [13], [20] across a wide photon energy range.

B. Attosecond Streaking

In attosecond streaking, the measurement consists in recording the final momentum of the photoelectrons after their ionization by the SAP and interaction with a few-cycle IR probe pulse for different pump-probe time delays. Depending on the value of the vector potential at their release time, the photoelectrons are accelerated to different final momenta, thus mapping time information onto the energy axis [21]–[23]. One of the first important applications of attosecond streaking was the complete characterization of the SAP by retrieving the XUV spectrum and phase via a retrieval algorithm called FROG-CRAB [24], [25].

In addition, two different spectrograms recorded simultaneously and composed by different types of electrons, for instance originating from different states of the same target or from different targets, can also yield relative timing information about the atomic photoionization delay.

Pioneering experiments conducted on solid [26] or gas targets [14] have revealed unexpected time delays. In [14] a time delay in atomic photo emission of about 20 as has been extracted between electrons ionized from the 2s shell of neon with respect to the 2p shell.

How can this relative timing information be inferred from streaking measurements? Two methods have been presented: a temporal relative shift along the delay axis between the spectrograms formed by 2s and 2p electrons can be interpreted as a relative delay [26]; alternatively, the group delays of both electron wavepackets can be retrieved from the spectrograms and their difference computed at the relative peak position [14].

However, as we will show in the next sections, in both these methods the role of the temporal structure of the ionizing SAP (i.e., attochirp) has not been considered in detail. After introducing the experimental setup, we will show that the XUV attochirp may greatly influence the measurement and present a procedure how to retrieve reliable energy-dependent time delays from streaking measurements even if the SAPs are chirped.

III. Attosecond Streaking in Coincidence

A. Experimental Setup

The experimental setup is described in detail elsewhere [27]. We record attosecond streaking traces for two different target species, argon and neon, simultaneously, by exploiting the coincidence capability of a reaction microscope [28], [29] detector. We prepare a gas target containing a proper mixture of argon

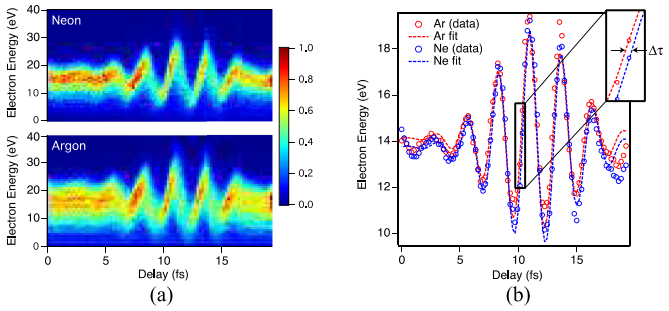

Fig. 1. (a) Streaking photoelectron spectrograms obtained from photoelectrons originating from simultaneous ionization of neon and argon. (b) Time dependent center-of-mass energy shift extracted from the spectrograms (open circles) for argon (red) and neon (blue) with corresponding fit (dashed line).

and neon such that in every measurement the experimental conditions for both noble gases are identical. This ensures that systematic errors in the determination of photo ionization time delays are reduced to the minimum because electrons coming from both species see exactly the same XUV and IR fields. The gas target mixture is ionized with SAPs of 10-eV-bandwidth centered at about 35 eV. A moderately strong (about 3×10^{12} W/cm^2) IR pulse with controllable delay modulates the final photoelectron momentum by streaking the electrons in the continuum according to the instantaneous magnitude of the vector potential.

The SAP is generated by focusing 800-nm IR laser pulses, with a duration of approximately 5 fs and their polarization shaped by a polarization gating scheme [30] into an argon gas target. The XUV-pump beam is first recombined with the delayed IR-probe through a holey mirror and both beams are subsequently collinearly focused by a toroidal mirror into a supersonic gas target, which is located inside the reaction microscope.

Ions and electrons are separated by a dc electric field and guided towards space and time sensitive detectors. This allows retrieving not only the kinetic energy of each individual particle at the moment of ionization but also their 3-D momentum vector. Applying a coincidence filter of the time of flight of the parent ions allows distinguishing between electrons originating from the photoionization of argon or neon, even though they energetically overlap.

B. Center-of-Mass Analysis

The two separate streaking traces obtained by this procedure for a mixture of argon and neon are shown in Fig. 1(a). In a first approach, the timing information can be readily retrieved by quantifying the relative shift between the two streaking curves along the time axis [26]. We calculate the center-of-mass of the photoelectron energies between 0 and 40 eV (blue and red open circles of Fig. 1(b) and we fit the curves with the following formula representing an analytic form of the IR vector potential:

$$G = Ae^{-\frac{(\tau-\tau_0)}{2\sigma^2}} \cos\left[\omega_{\mathrm{IR}}\left(\tau-\tau_0\right)-\varphi\right]. \tag{3}$$

The photo ionization time delay between the two species can be extracted from the difference between the phases φ^{Ar} and φ^{Ne} for argon and neon, respectively:

$$\Delta\tau^{\mathrm{Ar/Ne}} = \tau^{\mathrm{Ar}} - \tau^{\mathrm{Ne}} = \frac{\varphi^{\mathrm{Ar}} - \varphi^{\mathrm{Ne}}}{\omega_{\mathrm{IR}}}. \tag{4}$$

This procedure yields a time delay difference $\Delta\tau^{\mathrm{Ar/Ne}} = -82$ as. Since the sign convention is such that positive values correspond to delayed emission, the result shown in Fig. 1 indicates that the emission of photoelectrons from neon is delayed relative to that from argon.

C. FROG-CRAB Retrieval Algorithm

The analysis based on the calculation of the center-of-mass in energy returns a time delay difference $\Delta\tau^{\mathrm{Ar/Ne}}$ averaged across the whole bandwidth of the photoelectron spectrum. In this way, we compare photoelectron energies, without information about which XUV photon energy was absorbed by each photoelectron.

From a physical point of view, this means that we are also attributing the delay contribution due to a possible attochirp of the XUV pump pulse to the photo ionization atomic time delay. In other words, we are stopping but not starting the clock at the same time for all the electrons: an apparent delay between two photoelectrons may arise simply because they started at different instances of time within the attosecond pulse.

The solution for this ambiguity is to compute time delay differences between photoelectrons ionized by the XUV photons of the same energy. However, this is not as straightforward as with the RABBITT technique as discussed in Section II-A. With RABBITT we use an APT with discrete harmonics in the energy spectrum of the XUV pulses which allows for a straightforward identification between electron kinetic energy and XUV photon energy. For the streaking technique the situation is more complicated because a SAP instead of an APT is used which produces a continuum in the XUV pulse spectrum.

It is often assumed that the photoelectron spectrum is a replica of the XUV spectrum, just shifted in energy by the ionization potential of the target. But this is true only in the case of a uniform spectral response of the target to the ionizing photon energy, which is reflected by an energy independent absorption cross section within the energy bandwidth of the XUV pulse. In general, however, absorption cross sections may be frequency dependent such that the target atom absorbs photons of certain energy more likely than others. Thus the SAP spectrum can be enhanced or suppressed resulting in an apparent shift in energy of the photoelectron spectrum as compared to the simple photo ionization formula $E_{\mathrm{kin}} = \hbar\omega_{\mathrm{XUV}} - I_p$, where E_{kin} is the kinetic energy of the photoelectron ionized by a photon of frequency ω_{xuv} and I_p is the ionization potential.

In a streaking experiment, under certain assumptions, it is possible to retrieve information about the phase of the XUV spectrum: it is contained in the spectrogram itself and can be extracted applying the FROG-CRAB retrieval algorithm.

The foundations of this technique are based on the strong field approximation (SFA): the measured spectrogram intensity $I(\mathbf{p},t)$ for an electron with momentum $\mathbf{p}$ at a delay τ between the XUV pump and the IR probe can be written as (atomic units are

used) [25]:

$$I(\mathbf{p},\tau) = \left| \int_{-\infty}^{\infty} F_{\mathrm{XUV}}(t-\tau)\, \mathbf{d_p} \exp\left(i\phi_L(t,\mathbf{p})\right) \exp\left[i\left(\mathbf{p}^2/2 + I_p\right)t\right] dt \right|^2 \quad (5)$$

with

$$\phi_L(t,\mathbf{p}) = -\int_t^{\infty} \left[\mathbf{p}\cdot\mathbf{A_L} + A_L^2(t')/2\right] dt' \quad (6)$$

where $\mathbf{d_p}$ is the transition dipole matrix element connecting the bound (ground) state with the continuum, $F_{\mathrm{XUV}}(t)$ is the electric field of the XUV pulse and $\mathbf{A_L}(t)$ is the vector potential of the IR field pulse.

Some approximations are adopted to simplify the problem. First, it is assumed that the electron pulse created in the continuum by the transition dipole matrix element $\mathbf{d_p}$ is an exact replica of the attosecond XUV spectrum. In other words $\mathbf{d_p}$ is set equal to 1. Second, the final momentum of the electron $\mathbf{p}$ is approximated with the central momentum $\mathbf{p_c}$ of the unstreaked photoelectron spectrum. Third, the equation is reduced to one dimension, which is valid for experiments where the electrons are collected within a small solid angle around the IR polarization axis.

The 1-D approximation is particularly important if the streaking experiments are performed with a reaction microscope or other detectors with 3-D momentum resolution. In this case also electrons emitted with a large angle with respect to the XUV (and IR) polarization direction are detected, thus preventing a reliable reconstruction from the full data set. In Ref [31] it has been shown that the retrieval algorithm is still trustful for electron counts collected within a cone with a full opening angle up to 40°. However, for all the measurements presented here a filter to the electrons was used selecting only the counts lying within 20°, thus ensuring a precise reconstruction and an adequate amount of usable counts.

With the three approximations summarized above Eq. (5) and (6) become:

$$I(p,\tau) = \left| \int_{-\infty}^{\infty} F_{\mathrm{XUV}}(t-\tau) \exp\left(i\phi_L(t)\right) \exp\left[i\left(p^2/2 + I_p\right)t\right] dt \right|^2 \quad (7)$$

and

$$\phi_L(t) = -\int_t^{\infty} \left[p_c A_L + A_L^2(t')/2\right] dt'. \quad (8)$$

It can be shown that $I(p, \tau)$ is represented by a pair of F_{XUV} and A_L. Therefore, using an iterative procedure such as the generalized projection algorithm allows extracting the spectrum (and the phase) of the XUV pump pulse as well as the shape of the IR probe field [24], [25]. This is the procedure that is normally adopted in order to characterize SAPs. However, if two streaking traces are measured simultaneously, the difference in spectral phases retrieved with this method gives also access to the timing information about the photo ionization process itself with high accuracy [14], [25].

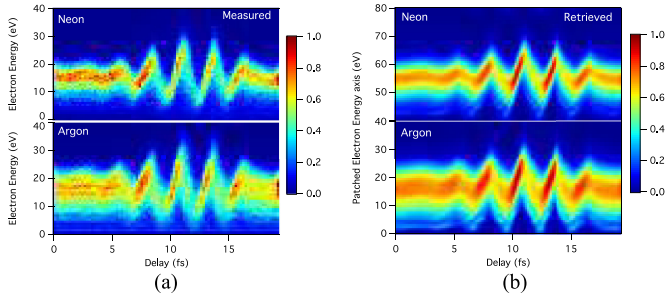

Fig. 2. Measured (a) and reconstructed spectrograms (b) for argon and neon photoelectrons. In the experiments, only electrons with a final momentum having an angle smaller than 20° with respect to the XUV and IR polarization direction are considered.

D. XUV Spectrum and Group Delay Retrieval With FROG-CRAB

In this section we will explain in more details how to retrieve the phase information. The spectral phase extracted using the above procedure can be expanded in a Taylor series around the central frequency of the pulse ω_0:

$$\phi(\omega) = \phi(\omega_0) + \sum_{n=1}^{\infty} \frac{1}{n!} \left.\frac{\partial^n \phi}{\partial \omega^n}\right|_{\omega_0} (\omega-\omega_0)^n. \quad (9)$$

The zero-order term $\phi(\omega_0)$ determines the overall phase of the pulse, the first-order is the group delay and the second order represents the group delay dispersion of the pulse.

We can rewrite equation (9) introducing a function $\theta(\omega)$ containing phase terms of order higher than the second:

$$\phi(\omega) = \phi(\omega_0) + \left.\frac{\partial \phi}{\partial \omega}\right|_{\omega_0} (\omega-\omega_0) + \frac{1}{2}\left.\frac{\partial^2 \phi}{\partial \omega^2}\right|_{\omega_0} (\omega-\omega_0)^2 + \int \theta(\omega)\, d\omega.$$

The group delay τ_{GD} is defined as

$$\tau_{\mathrm{GD}} \doteq \frac{\partial \phi}{\partial \omega} = \left.\frac{\partial \phi}{\partial \omega}\right|_{\omega_0} + \left.\frac{\partial^2 \phi}{\partial \omega^2}\right|_{\omega_0} (\omega-\omega_0) + \theta(\omega) = \tau_0 + \alpha(\omega_0)(\omega-\omega_0) + \theta(\omega). \quad (10)$$

In equation (10), we see that neglecting the higher orders contained in the function $\theta(\omega)$, the group delay is given by a straight line with offset τ_0 and a slope given by $\partial^2\phi/\partial\omega^2$ representing the chirp of the XUV pulse.

The zero-order term τ_0 includes an offset t_0, which can be set arbitrarily in the reconstruction. It represents the choice made for the absolute zero of the temporal frame and affects the retrieved τ_{GD}. However, if two streaking traces are processed simultaneously, the reconstruction refers to a unique time axis. Therefore the offset term t_0 cancels out when the difference between time delays $\tau_{\mathrm{GD}}^{(1)} - \tau_{\mathrm{GD}}^{(2)}$ is computed.

Fig. 2 shows the measured (panel (a)) and retrieved (panel (b)) argon and neon spectrograms. Before running the FROG-CRAB retrieval algorithm, the experimental traces are patched together at an arbitrarily chosen energy of 40 eV in order to process

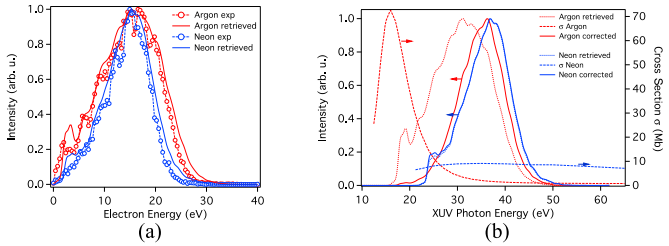

Fig. 3. (a) The argon and neon spectra (solid red and blue line, respectively) retrieved from the streaking traces shown in Fig. 1(a) agree quite well with the measured IR-unperturbed photoelectron spectra (open circles with dashed line, red for argon, blue for neon). (b) The same spectra as (a) are shown shifted according to the different ionization potentials of argon and neon (red and blue dotted lines). If the corresponding photoabsorption cross-sections (dashed lines) are considered, the corrected spectra (red solid line for argon, blue dashed line for neon) are quite similar and in particular peak at the same XUV photon energy of about 37 eV.

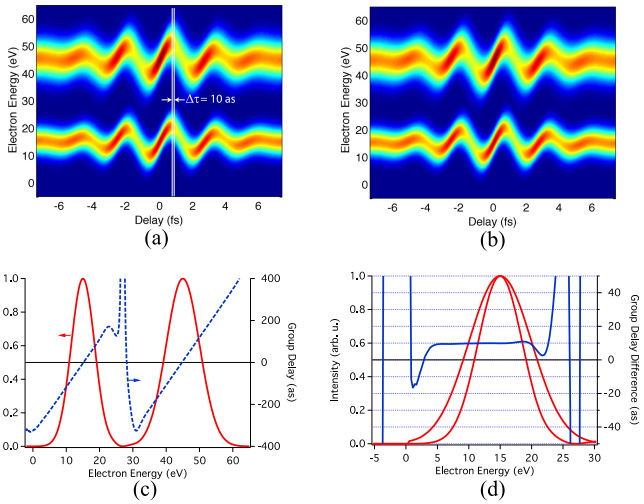

Fig. 4. (a) Simulated attosecond streaking traces prepared with the same chirp and a time delay of 10 as. (b) Reconstructed traces as obtained by the FROG-CRAB algorithm. (c) Retrieved spectra and group delays $\tau_{\mathrm{GD}}^{\mathrm{up}}$ and $\tau_{\mathrm{GD}}^{\mathrm{low}}$ for both spectrograms. (d) The initial group delay of 10 as is retrieved over the whole bandwidth of the spectra.

both spectrograms simultaneously. After the reconstruction, the spectra and phases are disentangled by shifting the neon data back to their original spectral position.

Fig 3(a) shows the spectra for argon and neon (solid line) retrieved from the spectrograms of Fig. 2. They are compared with the measured IR-unperturbed spectra, obtained by integrating the counts of Fig. 2(a) within the first 2 fs of the pump-probe scan and the agreement between the traces is excellent.

Interestingly, even though the photoelectron spectra for the two target species are created by the same XUV pulse and acquired simultaneously, Fig. 3(b) shows that the XUV spectrum retrieved from argon electrons is about 40% broader and peaks at an energy 6 eV lower with respect to the spectrum obtained from neon electrons.

These features can be explained if the photoabsorption cross-section of the different targets is taken into account. Indeed, while the neon cross-section is almost flat over the bandwidth of the pulse, the argon cross-section exhibits a strongly non-uniform behavior (see Fig. 3(b)), such that electrons counts at low kinetic energies are enhanced. This explains also why the offset of the center-of-mass shift, shown in Fig. 1(b), is almost at the same value of about 14 eV for both targets even though the relative ionization energies differ by about 6 eV.

The spectra corrected with the corresponding photoabsorption cross-sections (see Fig. 3(b)) are quite similar with a residual small discrepancy in peak position of 1 eV only.

Before showing the spectral phases retrieved by the FROG-CRAB algorithm from the two experimental traces shown in Fig. 1(a), it is worth testing with some simulated spectrograms whether the procedure yields reliable results.

Fig. 4(a) shows two simulated streaking spectrograms prepared with different spectral bandwidth, same amount of chirp and shifted in time by a small delay $\Delta\tau$ of 10 as. Such traces are similar to the ones measured experimentally shown in Fig. 1(a), where argon and neon valence electrons are ionized by the same attosecond XUV pulse and streaked by the same IR field.

The time delay between the two traces is calculated as the difference between the two group delays referred to as $\tau_{\mathrm{GD}}^{\mathrm{up}}$ and $\tau_{\mathrm{GD}}^{\mathrm{low}}$ for the upper and lower trace, respectively. The latter are determined through the derivative of the retrieved spectral phase as already shown in Eq (10):

$$\Delta\tau_{\mathrm{GD}} = \tau_{\mathrm{GD}}^{\mathrm{up}} - \tau_{\mathrm{GD}}^{\mathrm{low}} = \hbar\left(\frac{\partial\varphi^{\mathrm{up}}}{\partial E} - \frac{\partial\varphi^{\mathrm{low}}}{\partial E}\right). \qquad (11)$$

Fig. 4(d) shows that the FROG-CRAB algorithm reliably reconstructs the time delay of 10 as over the whole bandwidth of the spectra.

IV. Attochirp Corrected Photoionization Time Delays

After showing that the FROG-CRAB algorithm reliably reproduces the measured photoelectron spectrum (see Fig. 3) and determines with high precision the difference in group delays between two electron wavepackets streaked by the same IR field (see Fig. 4), we are now in place to retrieve the energy-dependent photoionization time delay difference between argon and neon as shown in Fig. 5.

In Fig. 5(a), we can see that for both target atoms the slope of the group delay curve is quite steep, on the order 25 as/eV, indicating that the XUV pump pulse is relatively strongly chirped.

If we compute the time delay difference between the two species $\Delta\tau^{\mathrm{Ar/Ne}} = \tau_{\mathrm{GD}}^{\mathrm{Ar}} - \tau_{\mathrm{GD}}^{\mathrm{Ne}}$ for photoelectrons having the same kinetic energy $\Delta E_{\mathrm{kin}} = E_{\mathrm{kin}}^{\mathrm{Ar}} - E_{\mathrm{kin}}^{\mathrm{Ne}} = 0$ (as indicated by the black vertical line in Fig. 5(a) for the case of 12 eV electron kinetic energy), we obtain a value of $\Delta\tau^{\mathrm{Ar/Ne}} \approx -90$ as. However, it was already shown with the help of Fig. 2 that this procedure does not ensure that Argon and Neon photoelectrons have been ionized by XUV photons of the same energy ($\Delta E_{\mathrm{XUV}} = E_{\mathrm{XUV}}^{\mathrm{Ar}} - E_{\mathrm{XUV}}^{\mathrm{Ne}} \neq 0$) and therefore does not eliminate the contribution to the delay introduced by the attochirp.

This method of extracting time delay differences is equivalent to the center-of-mass analysis presented above, and indeed, the value for $\Delta\tau^{\mathrm{Ar/Ne}} = -85$ as that we would obtain calculating the average of the individual time delay differences within the spectral bandwidth agrees very well with the estimation provided by the center-of-mass analysis $\Delta\tau^{\mathrm{Ar/Ne}} = -82$ as.

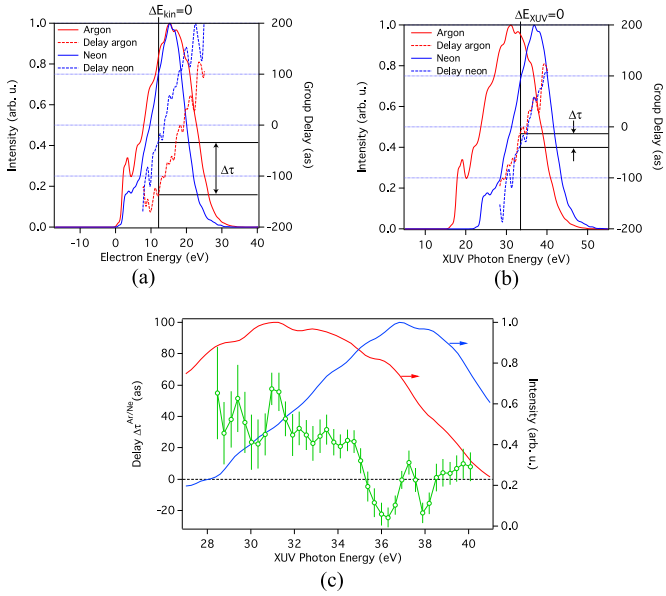

Fig. 5. (a) Spectra and group delays for argon and neon retrieved with the FROG-CRAB algorithm from the experimental traces shown in Fig. 1(a). The vertical and horizontal black lines indicate that comparing the group delays for both species at the same photoelectron energy results in a time delay difference $\Delta\tau^{\mathrm{Ar/Ne}} \approx -90$ as for an electron kinetic energy of about 12 eV. (b) Same as (a) but with the spectrograms shifted by the ionization potential of the two targets. Comparing group delays for both species at the same XUV photon energy results in a time delay difference $\Delta\tau^{\mathrm{Ar/Ne}} \approx +30$ as for a photon energy of about 32 eV. (c) For any XUV energy within a range where the spectral intensity of the argon spectrum (red solid line) and neon spectrum (blue solid line) overlap, a time delay $\Delta\tau^{\mathrm{Ar/Ne}}$ is extracted. The green open circles represent the mean value of 33 independent measurements while the error bars represent the standard deviation of the mean value.

The key to obtain attochirp-corrected time delays in attosecond energy streaking is to compute $\Delta\tau^{\mathrm{Ar/Ne}}$ at the same XUV photon energy, such that $\Delta E_{\mathrm{XUV}} = 0$ even if $\Delta E_{\mathrm{kin}} \neq 0$ (see black vertical line in Fig. 5(b)). The photoelectron spectra and group delays depicted in Fig. 5(a) are first shifted in energy according to the different ionization potential of the two species, thus retrieving the photon spectra as shown in Fig. 3. Then, for any photon energy within the range where the spectral intensity of both spectra overlap, the difference between the group delays retrieved for argon and neon can be computed, yielding the energy-dependent delay curve presented in Fig. 5(c).

For the considered energy range the difference $\Delta\tau^{\mathrm{Ar/Ne}}$ is mainly positive, a result completely opposite to the one obtained by the COM analysis, where the contribution to the delay given by the attochirp is not eliminated. While the residual attochirp in our pulses was rather strong, it is important to note that even a more moderate attochirp will introduce significant systematic errors if the analysis is not done properly.

V. Conclusion

In conclusion, we have shown a detailed description of how to extract photoionization time delay differences between two types of electrons emitted from two different targets when attosecond energy streaking is employed. We have shown that any attochirp of the SAP manifests itself in the same way as the atomic photoionization time delay and therefore can lead to wrong interpretations if it is not properly taken into account. Our measurements give access to the photoionization time delay difference between electrons originating from argon with respect to those ionized by neon. Our experiments yield delays of a few tens of attoseconds in a XUV photon energy range between 28 and 38 eV.

Acknowledgment

M. Lucchini would like to thanks the ETH Zurich Postdoctoral Fellowship Program for support.

References

[1] P. M. Paul *et al.*, "Observation of a train of attosecond pulses from high harmonic generation," *Science*, vol. 292, pp. 1689–1692, 2001.
[2] R. Kienberger *et al.*, "Atomic transient recorder," *Nature*, vol. 427, pp. 817–821, 2004.
[3] F. Krausz and M. Ivanov, "Attosecond physics," *Rev. Mod. Phys.*, vol. 81, p. 163, 2009.
[4] L. Gallmann, C. Cirelli, and U. Keller, "Attosecond science: Recent highlights and future trends," *Annu. Rev. Phys. Chem.*, vol. 63, pp. 447–469, 2012.
[5] Z. H. Chang and P. Corkum, "Attosecond photon sources: the first decade and beyond," *J. Opt. Soc. Amer. B*, vol. 27, pp. B9–B17, Nov. 2010.
[6] A. Maquet, J. Caillat, and R. Taïeb, "Attosecond delays in photoionization: Time and quantum mechanics," *J. Phys. B, Atomic Mol. Opt. Phys.*, vol. 47, 2014.
[7] P. Eckle *et al.*, "Attosecond ionization and tunneling delay time measurements in helium," *Science*, vol. 322, pp. 1525–1529, 2008.
[8] P. Eckle *et al.*, "Attosecond angular streaking," *Nature Phys.*, vol. 4, pp. 565–570, 2008.
[9] E. Goulielmakis *et al.*, "Single-cycle nonlinear optics," *Science*, vol. 320, pp. 1614–1617, 2008.
[10] H. G. Muller, "Reconstruction of attosecond harmonic beating by interference of two-photon transitions," *Appl. Phys. B*, vol. 74, pp. S17–S21, 2002.
[11] A. S. Landsman *et al.*, "Ultrafast resolution of tunneling delay time," *Optica*, vol. 1, pp. 343–349, 2014.
[12] A. S. Landsman and U. Keller, "Attosecond science and the tunneling time problem," *Phys. Rep.*, vol. 547, pp. 1–24, 2015.
[13] K. Klünder *et al.*, "Probing single-photon ionization on the attosecond time scale," *Phys. Rev. Lett.*, vol. 106, p. 143002, 2011.
[14] M. Schultze *et al.*, "Delay in photoemission," *Science*, vol. 328, pp. 1658–1662, Jun 2010.
[15] J. M. Dahlström, A. L'Huillier, and A. Maquet, "Introduction to attosecond delays in photoionization," *J. Phys. B Atomic Mol. Opt. Phys.*, vol. 45, 2012.
[16] C. Iaconis and I. A. Walmsley, "Spectral phase interferometry for direct electric field reconstruction of ultrashort optical pulses," *Opt. Lett.*, vol. 23, pp. 792–794, 1998.
[17] F. T. Smith, "Lifetime matrix in collision theory," *Phys. Rev.*, vol. 118, pp. 349–356, 1960.
[18] E. P. Wigner, "Lower limit for the energy derivative of the scattering phase shift," *Phys. Rev.*, vol. 98, p. 145, 1955.
[19] R. Locher *et al.*, "Versatile attosecond beamline in a two-foci configuration for simultaneous time-resolved measurements," *Rev. Sci. Instrum.*, vol. 85, pp. 013113-1–013113-2, 2014.
[20] D. Guénot *et al.*, "Photoemission-time-delay measurements and calculations close to the 3s-ionization-cross-section minimum in Ar," *Phys. Rev. A*, vol. 85, 2012.
[21] J. Itatani *et al.*, "Attosecond streak camera," *Phys. Rev. Lett.*, vol. 88, p. 173903, 2002.
[22] M. Kitzler, N. Milosevic, A. Scrinzi, F. Krausz, and T. Brabec, "Quantum theory of attosecond XUV pulse measurement by laser-dressed photoionization," *Phys. Rev. Lett.*, vol. 88, p. 173904, 2002.
[23] R. Kienberger *et al.*, "Steering attosecond electron wave packets with light," *Science*, vol. 297, pp. 1144–1148, 2002.
[24] Y. Mairesse and F. Quéré, "Frequency-resolved optical gating for complete reconstruction of attosecond bursts," *Phys. Rev. A*, vol. 71, p. 011401, 2005.

[25] J. Gagnon and V. S. Yakovlev, "The robustness of attosecond streaking measurements," *Opt. Exp.*, vol. 17, pp. 17678–17693, 2009.
[26] A. L. Cavalieri *et al.*, "Attosecond spectroscopy in condensed matter," *Nature*, vol. 449, pp. 1029–1032, 2007.
[27] M. Sabbar *et al.*, "Combining attosecond XUV pulses with coincidence spectroscopy," *Rev. Sci. Instrum.*, vol. 85, p. 103113, 2014.
[28] R. Dörner *et al.*, "Cold target recoil ion momentum spectroscopy: A "momentum microscope" to view atomic collision dynamics," *Phys. Rep.*, vol. 330, pp. 95–192, Jun. 2000.
[29] J. Ullrich *et al.*, "Recoil-ion and electron momentum spectroscopy: Reaction-microscopes," *Rep. Prog. Phys.*, vol. 66, pp. 1463–1545, 2003.
[30] I. J. Sola *et al.*, "Controlling attosecond electron dynamics by phase-stabilized polarization gating," *Nature Phys.*, vol. 2, pp. 319–322, 2006.
[31] H. Wang *et al.*, "Practical issues of retrieving isolated attosecond pulses," *J. Phys. B, Atomic Mol. Opt. Phys.*, vol. 42, p. 134007, 2009.

Claudio Cirelli was born in Milan, Italy, on April 28, 1977. He received the master's degree in physics from Milan University, Milan, in February 2002, and the Ph.D. degree in the Surface Physics Group of Prof. Jürg Osterwalder, University of Zurich, Zurich, Switzerland, in December 2006.

From 2007 to March 2013, he was a Postdoctoral Researcher in the Group of Prof. Ursula Keller (Ultrafast Laser Physics), Eidgenössische Technische Hochschule, Zurich, where he is currently a Oberassistant (Senior Scientist). His research interests include broad areas of ultrafast spectroscopy with particular interest on attosecond science, strong-field interactions of light with matter, and ultrafast lasers and technology.

Mazyar Sabbar was born in Tehran, Iran, on September 21, 1983. He received the Dipl.Phys. degree from the Leibniz University of Hanover, Hanover, Germany, in 2010, and the Ph.D. degree from the Prof. Ursula Keller's Group, Eidgenössische Technische Hochschule, Zurich, Switzerland, in 2014, for his attosecond time-resolved studies conducted on a coincidence detector.

Since 2014, he has been a Postdoctoral Fellow in the Group of Prof. Stephen Leone, University of California, Berkeley, CA, USA. His current research interests include correlated electron dynamics occurring on time scales of attoseconds to few-femtoseconds in atomic and molecular systems.

Sebastian Heuser was born in Marburg, Germany, on January 15, 1987. He received the Dipl.Phys. degree from the Ruprecht-Karls-Universität in Heidelberg, Germany, in 2011. He is currently working toward the Ph.D. degree in the group of Prof. Ursula Keller (Ultrafast Laser Physics), Eidgenössische Technische Hochschule, Zurich, Switzerland.

His current research interests include exploring anisotropic effects in the attosecond timing of atomic photoionization and the influence of electron correlation on the photoelectron dynamics of molecular hydrogen.

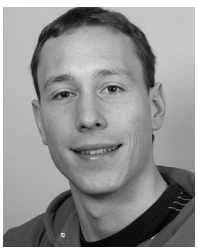

Robert Boge was born in Hamburg, Germany, on January 20, 1987. He received the master's degree in physics from the University of Massachusetts Amherst, Amherst, MA, USA, in September 2010. He joined the Prof. Ursula Keller's Group (Ultrafast Laser Physics), Eidgenössische Technische Hochschule, Zurich, Switzerland, in 2010, and received the Ph.D. degree in October 2014. He is currently a High Power Beam Diagnostic Specialist with the Extreme Light Infrastructure, Prague, Czech Republic. His research interests include ultrafast laser diagnostics, ultrafast spectroscopy, and attosecond science.

Matteo Lucchini was born in Angera, Italy, on January 29, 1984. He received the master's degree in physical engineering (*cum laude*) and the Ph.D. degree in physics in Prof. Mauro Nisoli's Group from the Politecnico di Milano, Milano, Italy, in December 2008 and March 2012, respectively.

From September 2009 to October 2009, he was a Visitor with Prof. Marc Vrakking's Group, AMOLF Institute, Amsterdam, The Netherlands. Since January 2012, he has been a Postdoctoral Fellow at the Ultrafast Laser Physics Group, Eidgenössische Technische Hochschule (ETH), Zurich, Switzerland, with Prof. Ursula Keller, where he received an ETH Fellowship Grant in June 2012. His current research interests include ultrafast spectroscopy, attosecond science, and its applicability to gas and solid targets.

Lukas Gallmann studied physics at the Eidgenössische Technische Hochschule (ETH), Zurich, Switzerland, where he received the Ph.D. degree in the generation and characterization of few-cycle optical pulses in the Ultrafast Laser Physics Group of Prof. Ursula Keller, in 2002. He joined a local aerospace company to work on laser-based intersatellite communication and on optical instrumentation for scientific space missions. In early 2005, he returned to academia as a Postdoctoral Fellow with Lawrence Berkeley National Laboratory, Berkeley, CA, USA, and the University of California in Berkeley, Berkeley, where he entered the field of attosecond science. In 2006, he rejoined the Ultrafast Laser Physics Group, ETH, where he became responsible for coordinating the attosecond activities of the group. He has published more than 50 papers. His research interests include new few-cycle sources and techniques for attosecond science and their application to relevant physical problems at the frontier of ultrafast science. For his work on new sources and techniques in attosecond science, he received the habilitation in 2012.

Ursula Keller (F'14) received the Dipl.Phys. degree from Eidgenössische Technische Hochschule (ETH) Zurich, Zürich, Switzerland, in 1984, and the Ph.D. degree in applied physics from Stanford University, Stanford, CA, USA, in 1989.

She was a Member of the Technical Staff with AT&T Bell Laboratories, Murray Hill, NJ, USA, from 1989 to 1993. She was a Visiting Miller Professor with the University of California, Berkeley, CA, in 2006, and a Visiting Professor at the Lund Institute of Technologies, Sweden, in 2001. She joined ETH Zurich as a Tenured Professor of physics in 1993 and has been a Director of the NCCR MUST since 2010. She has been a Cofounder and a Board Member for Time-Bandwidth Products acquired by JDSU, in 2014, and GigaTera, from 2000 to 2003, adventure capital funded telecom company during the "bubble phase," which was acquired by Time-Bandwidth in 2003. She has published more than 380 peer-reviewed journal papers and many book chapters and patents. Her current research interests include exploring and pushing the frontiers in ultrafast science and technology.

She received the Charles Hard Townes Award of OSA 2015, the Arthur L. Schawlow Award 2013, which is the highest achievement award of the Laser Institute of America, the ERC advanced grant in 2012, the EPS Senior Prize in 2011, the OSA Fraunhofer/Burley Prize in 2008, the Philip Morris Research Award in 2005, the first-place award of the Berthold Leibinger Innovation Prize in 2004, and the Carl Zeiss Research Award in 1998.

She is a Fellow of the OSA, the EPS, and the SPIE.